Relaxation time of the nanomagnet Fe_4

E. Rastelli* and A. Tassi
Dipartimento di Fisica dell'Università, Parco Area delle Scienze 7/A, 43100 Parma, Italy
(Received 16 September 2008; revised manuscript received 28 January 2009; published 13 March 2009)

The magnetic behavior of the molecular nanomagnet Fe_4 is very well simulated by a single-spin model Hamiltonian in a crystal field with $S=5$. The crystal-field parameters were determined from the inelastic neutron scattering spectra. Here we show that the quantum effects are crucial to understand the saturation of the relaxation time observed at very low temperature at variance with the standard master equation result that leads to an Arrhenius law at any temperature. Very deep downward spikes in correspondence to the anticrossing fields are found in the relaxation time vs field at low temperature. We compare our results with those obtained by previous approaches worked out to fit experimental data on Mn_{12}.

DOI: 10.1103/PhysRevB.79.104415 PACS number(s): 75.45.+j, 75.50.−y

I. INTRODUCTION

An expanding area of the magnetism concerns the single-molecule magnets (SMMs) (Ref. 1) with slow relaxation of the magnetization at low temperature. Many interesting basic properties as magnetic quantum tunneling (MQT) as well as possible technical application in quantum computing or magnetic storage make the SMMs particularly attractive.

We focus on the tetrairon cluster $Fe_4(thme)_2(dpm)_6$ (briefly Fe_4)[2] where thme indicates the triply deprotonated 1,1,1-tris(hydroxylmethyl)ethane H_3thme and dpm indicates the deprotonated dipivaloylmethane Hdpm. The complete chemical formula of the tetrairon cluster reads $C_{76}H_{132}O_{18}Fe_4$.

The tetrairon cluster Fe_4 is a puzzle for theoretical physicists because the fit with experimental data of inelastic neutron scattering (INS) (Ref. 3) implies the existence of a term in the crystal-field Hamiltonian that violates the D_3 symmetry of the molecule as deduced by a single-crystal x-ray study[2] performed at $T=100$ K. The existence of such a symmetry-violating term may be ascribed to two different sources:

(i) The x-ray study at $T=100$ K established that the Fe_4 ions of the iron cluster are placed on the vertices and at the center of an equilateral triangle (D_3 symmetry); however, a small distortion of the equilateral to isosceles triangle, as suggested by Carretta *et al.*[3] could violate the D_3 symmetry. Rastelli and Tassi[4] proved that a distortion of less than half degree away from the equilateral symmetry is able to recover the term used in the fit with INS experiment. The distortion could be ascribed to a true distortion of the tetrairon cluster occurring at low temperature or the tolerance of the single-crystal x-ray study or the use of a powder sample in INS experiment.

(ii) If all the sources of possible distortion have to be excluded some not yet identified microscopic mechanism such as second-order Dzyaloshinshii-Moriya (DM) effects[5] might yield an effective term similar to that used by Carretta *et al.*[3] to fit INS data.

Experimental data in zero field[2] show that the relaxation time of magnetization of the tetrairon cluster Fe_4 shows an Arrhenius law for temperature $T \gtrsim 1$ K while saturation is found for $T \lesssim 0.2$ K, where thermal activation is negligible and quantum effects are dominant.

The theoretical approach to the relaxation time of the magnetization of a SMM is based on the master equation[6] in which the transition probability rates between the magnetic states are related to the spin-phonon interaction. For temperature high enough only thermal activation is accounted for[7] neglecting quantum tunneling. This approach leads to the Arrhenius law for the relaxation time vs temperature in good agreement with the experiment[8] on Mn_{12}. On the contrary in the very-low-temperature regime quantum effects are dominant, so that the relaxation time was evaluated by the Fermi golden rule at zero temperature[9] and the order of magnitude of the relaxation time of Mn_{12} in weak external magnetic field was recovered.

Then a generalized master equation[10] was proposed in order to account for the quantum tunneling at finite temperature. However, an approximation on the time dependence of the off-diagonal elements of the density matrix to reduce drastically the number of differential equations restricts the result to temperatures high enough. This calculation gave a satisfactory fitting of the experimental data on Mn_{12} between $T=1.9$ and 2.8 K explaining the deep downward spikes of the relaxation time as a function of the external magnetic field in correspondence to the fields at which the energy levels of the diagonal part of the crystal-field Hamiltonian cross each other. In this way the enhanced relaxation rate was correlated with the quantum tunneling in presence of spin-phonon interaction.

Until now an approach to describe the crossover from the pure quantum behavior in the low-temperature regime to the thermally activated regime, does not exist. We propose a generalized master equation (GME) suitable to describe both the quantum and the thermally activated regimes at any temperature and we use this approach to describe the relaxation time of the tetrairon cluster Fe_4. We have numerically diagonalized the crystal-field Hamiltonian in an external magnetic field and we have accounted for the temperature-dependent transition probability rates by the Fermi golden rule. The master equation we propose makes use of the main contributions to quantum tunneling selected by looking at the zero-temperature rigorous result.

We have also applied to Fe_4 a generalized master equation formalism similar to that used by Leuenberger and Loss[10] [Leuenberger and Loss master equation (LLME)] to evaluate the relaxation time of Mn_{12} at temperature high enough.

Good agreement between GME and LLME results is obtained for temperatures $T \gtrsim 2$ K. The scenario we find in Fe_4 is similar to that experimentally observed and theoretically investigated in Mn_{12}.[11] An overall decreasing of the relaxation time at increasing field is modified near the anticrossing fields by the presence of deep downward spikes. While the relaxation time at zero external field is heavily affected by both the hyperfine and the dipole fields, this is not the case at finite external field. For this reason we have considered the behavior of the tetrairon cluster Fe_4 in a nonzero external magnetic field and we support warmly an experiment to test our theoretical expectation.

II. TRANSITION PROBABILITY RATE

The monocrystal made up of tetrairon cluster Fe_4 is well simulated by an aggregate of noninteracting spins $S=5$ with crystal-field Hamiltonian

$$\mathcal{H}_s = \mathcal{H}_{cf} - g\mu_B H_z S_z, \tag{1}$$

where S_z is the component of the spin operator along the easy (z) axis, H_z is the magnetic field component along the easy axis, $g=2$ is the Landé g factor, μ_B is the Bohr magneton, and $\mathcal{H}_{cf}$ is the "zero-field splitting" Hamiltonian[3]

$$\mathcal{H}_{cf} = B_2^0 O_2^0 + B_4^0 O_4^0 + B_2^2 O_2^2 + B_4^3 O_4^3, \tag{2}$$

where B_n^m are anisotropy parameters and O_n^m are Stevens operator equivalents[12]

$$O_2^0 = 3S_z^2 - S(S+1), \tag{3}$$

$$O_4^0 = 35S_z^4 - [30S(S+1) - 25]S_z^2 - 6S(S+1) + 3[S(S+1)]^2, \tag{4}$$

$$O_2^2 = \frac{1}{2}(S_+^2 + S_-^2) \tag{5}$$

with $S_\pm = S_x \pm iS_y$ and

$$O_4^3 = \frac{1}{4}[S_z(S_+^3 + S_-^3) + (S_+^3 + S_-^3)S_z]. \tag{6}$$

The anisotropy parameters that give the best fit with both the inelastic neutron scattering data[3] and the hysteresis loop of the magnetization[2] were found to be[4] $B_2^0 = -0.216$, $B_4^0 = 1.16 \times 10^{-5}$, $B_2^2 = 0.014$ and $B_4^3 = 7 \times 10^{-4}$ K. The crystal structure is trigonal with lattice constants $a = 16.1893$ Å and $c = 52.172$ Å containing six molecules.[2]

From now on we will label $|m^*\rangle$ and ϵ_{m^*} the eigenstates and the eigenvalues of the crystal-field Hamiltonian of Eq. (1) and $|m\rangle$ and ϵ_m the eigenstates and the eigenvalues of the diagonal part of the crystal-field Hamiltonian obtained from Eq. (2) with $B_2^2 = B_4^3 = 0$. Since B_2^2 and B_4^3 are small with respect to the easy-axis anisotropy parameter B_2^0, it is expected that $|m^*\rangle$ and ϵ_{m^*} do not differ very much from $|m\rangle$ and ϵ_m, respectively. This is true over the whole spectrum of magnetic fields except very close to the anticrossing fields where two unperturbed eigenvalues ϵ_m and ϵ_n degenerate. At the anticrossing fields the true states $|m^*\rangle$ and $|n^*\rangle$ are given by $\sim \frac{1}{\sqrt{2}}(|m\rangle \pm |n\rangle)$.

To get the relaxation time of the SMM Fe_4, the monocrystal is initially saturated in a large negative magnetic field, so that each molecule is in the ground state $|-5^*\rangle \sim |-5\rangle$. For instance, for $H_z = -2$ T the ground state is $|-5^*\rangle = 0.999\,98|-5\rangle - 6.00 \times 10^{-3}|-3\rangle - 3.72 \times 10^{-3}|-2\rangle + \cdots$, where the dots mean the states $|m\rangle$ with $m \neq -5, -3, -2$; the weight of which is between 4×10^{-5} and 10^{-9}.

When the magnetic field is suddenly reversed the initial state is again a state $|-5^*\rangle \sim |-5\rangle$ (for instance, for $H_z = 0.05$ T one has $|-5^*\rangle = 0.999\,94|-5\rangle - 9.23 \times 10^{-3}|-3\rangle - 6.02 \times 10^{-3}|-2\rangle + \cdots$) but it is no longer the ground state which is now the state $|5^*\rangle \sim |5\rangle$ (for $H_z = 0.05$ T one has $|5^*\rangle = 0.999\,94|5\rangle - 8.99 \times 10^{-3}|-3\rangle - 5.85 \times 10^{-3}|2\rangle + \cdots$), so that the initial state relaxes into the ground state in a time τ owing to the interaction with lattice vibrations. A crucial role is played by the spin-phonon interaction Hamiltonian[9]

$$\mathcal{H}_{sp} = i\sum_{\boldsymbol{q},\lambda} \sqrt{\frac{\hbar}{2MN\omega_{\boldsymbol{q}\lambda}}} V_{\boldsymbol{q}\lambda}(\boldsymbol{S})(c_{\boldsymbol{q}\lambda} - c_{\boldsymbol{q}\lambda}^\dagger), \tag{7}$$

where $\hbar$ is the Planck's constant divided by 2π, the sum is performed over the wave vectors $\boldsymbol{q}$ of the Brillouin zone and over the phonon branches λ, N is the number of lattice cells, M is the mass of a Fe_4 molecule, $\omega_{\boldsymbol{q}\lambda}$ is the phonon dispersion relation of the branch λ, and $c_{\boldsymbol{q}\lambda}$ and $c_{\boldsymbol{q}\lambda}^\dagger$ are the destruction and creation operators of a phonon of wave vector $\boldsymbol{q}$ belonging to the branch λ. The spin-phonon potential interaction $V_{\boldsymbol{q}\lambda}(\boldsymbol{S})$ depends on the phonon variables $(\boldsymbol{q},\lambda)$ as well as on the spin $\boldsymbol{S}$ of the molecule Fe_4. The most general form for a trigonal lattice[13] is

$$\begin{aligned} V_{\boldsymbol{q}\lambda}(\boldsymbol{S}) = {} & [A_1(\boldsymbol{q},\lambda) + iA_2(\boldsymbol{q},\lambda)]S_-^2 + [A_1(\boldsymbol{q},\lambda) - iA_2(\boldsymbol{q},\lambda)]S_+^2 \\ & + [B_1(\boldsymbol{q},\lambda) + iB_2(\boldsymbol{q},\lambda)]\{S_-, S_z\} + [B_1(\boldsymbol{q},\lambda) \\ & - iB_2(\boldsymbol{q},\lambda)]\{S_+, S_z\}, \end{aligned} \tag{8}$$

where {,} means anticommutator and

$$A_1(\boldsymbol{q},\lambda) = \frac{1}{8} g_2 (q_x e_{\boldsymbol{q}\lambda}^x - q_y e_{\boldsymbol{q}\lambda}^y), \tag{9}$$

$$A_2(\boldsymbol{q},\lambda) = \frac{1}{8} g_2 (q_x e_{\boldsymbol{q}\lambda}^y + q_y e_{\boldsymbol{q}\lambda}^x), \tag{10}$$

$$B_1(\boldsymbol{q},\lambda) = \frac{1}{8}[(g_3 + g_4) q_x e_{\boldsymbol{q}\lambda}^z + (g_3 - g_4) q_z e_{\boldsymbol{q}\lambda}^x], \tag{11}$$

$$B_2(\boldsymbol{q},\lambda) = \frac{1}{8}[(g_3 + g_4) q_y e_{\boldsymbol{q}\lambda}^z + (g_3 - g_4) q_z e_{\boldsymbol{q}\lambda}^y]. \tag{12}$$

The magnetoelastic coupling constants g_2 and g_3 are connected with the lattice strain while g_4 is related to the lattice rotation;[9] $\boldsymbol{e}_{\boldsymbol{q}\lambda}$ is the polarization vector associated with the phonon $(\boldsymbol{q},\lambda)$.

The Fermi golden rule for the transition probability rate from a state $|n^* N\rangle$ to a state $|m^* N'\rangle$, where n^*, m^* are the labels characterizing the magnetic wave functions and N, N' are the labels describing the phonon quantum numbers, reads

$$W_{m^*,n^*} = \frac{2\pi}{\hbar} \sum_{N,N'} |\langle m^* N'|\mathcal{H}_{\rm sp}|n^* N\rangle|^2 p_N \delta(E_N - E_{N'} + \epsilon_{n^*} - \epsilon_{m^*}), \tag{13}$$

where E_N and $E_{N'}$ are the eigenvalues of the phonon Hamiltonian and p_N is the thermal weight of the initial phonon state $|N\rangle$. Using the spin-phonon Hamiltonian (7) one obtains

$$\begin{aligned} W_{m^*,n^*} = \frac{2\pi}{\hbar} \sum_{\boldsymbol{q},\lambda} \left(\frac{\hbar}{2MN\omega_{\boldsymbol{q}\lambda}}\right) |\langle m^*|V_{\boldsymbol{q}\lambda}(\boldsymbol{S})|n^*\rangle|^2 \\ \times [(1+n_{\boldsymbol{q}\lambda})\delta(\hbar\omega_{\boldsymbol{q}\lambda} + \epsilon_{m^*} - \epsilon_{n^*}) \\ + n_{\boldsymbol{q}\lambda}\delta(\hbar\omega_{\boldsymbol{q}\lambda} - \epsilon_{m^*} + \epsilon_{n^*})], \end{aligned} \tag{14}$$

where $n_{\boldsymbol{q}\lambda} = [e^{\beta\hbar\omega_{\boldsymbol{q}\lambda}} - 1]^{-1}$ is the thermal average of the phonon occupation number with $\beta = (k_B T)^{-1}$, where k_B is the Boltzmann constant and T is the absolute temperature. To perform the sum over λ and $\boldsymbol{q}$ in Eq. (14) we restrict ourselves to the three acoustic branches and to the long-wavelength region of the spectrum. Both restrictions are justified by the very low temperature at which the experiment on Fe_4 is performed ($T \lesssim 4$ K). Under the hypothesis that the tetrairon cluster behaves like an isotropic elastic medium in the long wave length limit, the dispersion relations become $\hbar\omega_{\boldsymbol{q}\lambda} = c_l q$ for $\lambda = 1$ and $\hbar\omega_{\boldsymbol{q}\lambda} = c_t q$ for $\lambda = 2,3$, where c_l and c_t are the sound velocities of longitudinal and transverse phonons, respectively. Under this assumption Eq. (14) gives

$$\begin{aligned} W_{m^*,n^*} = \frac{1}{96\pi\rho\hbar^4} \Bigg\{ \frac{g_2^2}{5}\left(\frac{2}{c_l^5} + \frac{3}{c_t^5}\right)(|\langle m^*|S_-^2|n^*\rangle|^2 + |\langle m^*|S_+^2|n^*\rangle|^2) \\ + \left[\frac{g_3^2}{5}\left(\frac{2}{c_l^5} + \frac{3}{c_t^5}\right) + \frac{g_4^2}{c_t^5}\right](|\langle m^*|\{S_-, S_z\}|n^*\rangle|^2 \\ + |\langle m^*|\{S_+, S_z\}|n^*\rangle|^2) \Bigg\} (\epsilon_{m^*} - \epsilon_{n^*})^3 n\left(\frac{\epsilon_{m^*} - \epsilon_{n^*}}{k_B T}\right), \end{aligned} \tag{15}$$

where $\rho = M/V_c$ is the density and $n(x) = (e^x - 1)^{-1}$. Note that for $\epsilon_{m^*} < \epsilon_{n^*}$ it is convenient to make use of the following identity:

$$(\epsilon_{m^*} - \epsilon_{n^*})^3 n\left(\frac{\epsilon_{m^*} - \epsilon_{n^*}}{k_B T}\right) = (\epsilon_{n^*} - \epsilon_{m^*})^3 \left[1 + n\left(\frac{\epsilon_{n^*} - \epsilon_{m^*}}{k_B T}\right)\right]. \tag{16}$$

Since there are no experimental data about the magnetoelastic constants g_n and the sound velocity c_l and c_t appearing in Eq. (15) we assume $g_2 \simeq g_3 \simeq g_4 = g$ and $c_l \simeq c_t = c$ so that the transition probability rate reads

$$W_{m^*,n^*} = A p(m^*, n^*) n\left(\frac{\epsilon_{m^*} - \epsilon_{n^*}}{k_B T}\right), \tag{17}$$

where

$$A = \frac{g^2}{96\pi\rho\hbar^4 c^5} \tag{18}$$

and

$$\begin{aligned} p(m^*, n^*) = [(\langle m^*|S_-^2|n^*\rangle)^2 + \langle n^*|S_-^2|m^*\rangle)^2 + 2(\langle m^*|\{S_-, S_z\} \\ \times |n^*\rangle)^2 + 2(\langle n^*|\{S_-, S_z\}|m^*\rangle)^2](\epsilon_{m^*} - \epsilon_{n^*})^3. \end{aligned} \tag{19}$$

The coupling constant $A = 1529$ K^{-3} s^{-1} is chosen to fit the relaxation time[2] $\tau = 1.7 \times 10^{-6}$ s at $T = 4$ K and $H_z = 0$ T.

III. RELAXATION TIME AT $T = 0$

From Eqs. (15) and (16) one sees that at $T = 0$ the only nonvanishing transition probability rates are $W_{m^*,-5^*}$ for which $\epsilon_{m^*} < \epsilon_{-5^*}$. The relaxation time is the inverse of the sum of all the transition probability rates from the initial state $|-5^*\rangle$ to the states $|m^*\rangle$; that is,

$$\tau = \frac{1}{\sum_{m^*} W_{m^*,-5^*}} \tag{20}$$

Even for magnetic fields far from the anticrossing fields where $|m^*\rangle \simeq |m\rangle$ the replacement of the eigenstates $|m^*\rangle$ with the eigenstates $|m\rangle$ leads to transition probability rates equal to zero and to an infinite relaxation time because of the nature of the spin-phonon interaction.

For $0 < H_z < H_1$, where $H_1 = 0.477$ T is the anticrossing field between the states $|4^*\rangle$ and $|-5^*\rangle$ corresponding to the minimum splitting $\Delta_{-5,4} = \epsilon_{-5^*}(H_1) - \epsilon_{4^*}(H_1)$, the state $|-5^*\rangle$ is the first excited state, so that the only nonzero transition probability rate is $W_{5^*,-5^*}$; that is,

$$W_{5^*,-5^*} = A \;\; p(-5^*, 5^*). \tag{21}$$

Note the crucial role played by the nondiagonal terms of the crystal-field Hamiltonian proportional to B_2^2 and B_4^3 that cause a mixing between the states $|m\rangle$. Indeed neglecting these terms, the eigenstates of the crystal-field Hamiltonian reduce to the states $|m\rangle$ and because of the nature of the spin-phonon coupling (8) the only nonvanishing transition probability rates are those between nearest levels ($W_{m\pm1,m}$) and next-nearest levels ($W_{m\pm2,m}$). This implies that the system starting from the state $|-5\rangle$ must overcome the energy barrier between the states $|-5\rangle$ and $|5\rangle$ to relax into the final state $|5\rangle$. This could happen only if the magnetic system *receives* energy from the phonon bath, an event impossible at $T = 0$ K, so that the relaxation time goes to infinity for $T \to 0$. On the contrary the weak mixing entered by B_2^2 and B_4^3 is sufficient to give a nonzero transition probability rate $W_{5^*,-5^*}$ corresponding to a direct quantum tunneling between states $|-5^*\rangle$ and $|5^*\rangle$ during which the magnetic system *gives* energy to the phonon bath, so that relaxation occurs even for $T \to 0$. For weak magnetic fields $\epsilon_{-5^*} - \epsilon_{5^*} \simeq 10 g \mu_B H_z$, so that $p(-5^*, 5^*) \propto H_z^3$ in agreement with the behavior expected[9] for the nanomagnet Mn_{12}.

In Table I we give $p(-5^*, m^*)$ for several magnetic fields. To get the relaxation time one has to sum the elements of each row, multiply the sum by $A = 1529$ K^{-3} s^{-1}, and take the inverse. As one can see from Table I the first column corresponding to $p(-5^*, 5^*)$ is complete since the ground-state energy ϵ_{5^*} is always below the initial state energy ϵ_{-5^*}. The second column corresponding to $p(-5^*, 4^*)$ appears at $H_1 = 0.477$ T, where also the energy ϵ_{4^*} becomes lower than

TABLE I. Transitions $p(-5^*,m^*)(K^3)$.

H_z(T)	$p(-5^*,5^*)$	$p(-5^*,4^*)$	$p(-5^*,3^*)$	$p(-5^*,2^*)$	$p(-5^*,1^*)$	$p(-5^*,0^*)$
0.1	1.24×10^{-8}					
0.2	1.06×10^{-7}					
0.3	4.05×10^{-7}					
0.4	1.24×10^{-6}					
0.5	6.37×10^{-6}	2.80×10^{-9}				
0.6	6.85×10^{-6}	4.85×10^{-7}				
0.7	1.74×10^{-5}	3.82×10^{-6}				
0.8	5.83×10^{-5}	2.21×10^{-5}				
0.9	5.09×10^{-4}	3.07×10^{-4}				
1	1.22×10^{-3}	1.61×10^{-3}	7.60×10^{-7}			
1.1	1.13×10^{-4}	5.16×10^{-4}	3.14×10^{-5}			
1.2	4.01×10^{-5}	8.72×10^{-4}	1.72×10^{-4}			
1.3	2.01×10^{-5}	2.97×10^{-3}	6.75×10^{-4}			
1.4	3.43×10^{-5}	4.30×10^{-2}	8.69×10^{-3}			
1.5	4.60×10^{-5}	3.48×10^{-2}	1.53×10^{-2}	1.55×10^{-4}		
1.6	1.68×10^{-5}	6.68×10^{-3}	1.01×10^{-2}	3.76×10^{-3}		
1.7	1.62×10^{-5}	3.84×10^{-3}	1.81×10^{-2}	1.99×10^{-2}		
1.8	3.22×10^{-5}	3.39×10^{-3}	5.33×10^{-2}	6.87×10^{-2}		
1.9	5.13×10^{-4}	6.47×10^{-3}	0.993	0.240		
2	1.56×10^{-4}	2.89×10^{-3}	0.130	0.555	1.19×10^{-3}	
2.1	1.58×10^{-4}	5.05×10^{-3}	2.68×10^{-2}	1.53	1.34×10^{-2}	
2.2	4.19×10^{-4}	1.08×10^{-2}	3.03×10^{-2}	5.11	4.76×10^{-2}	
2.3	2.04×10^{-3}	4.06×10^{-2}	0.104	27.4	0.138	
2.4	0.267	4.29	10.1	3.80×10^{3}	17.9	
2.5	6.13×10^{-3}	8.61×10^{-2}	0.172	90.5	2.43	0.175
2.6	1.90×10^{-3}	2.67×10^{-2}	5.17×10^{-2}	28.7	3.59	1.94
2.7	1.16×10^{-3}	2.15×10^{-2}	5.89×10^{-2}	18.8	9.66	8.34
2.8	9.82×10^{-4}	4.78×10^{-2}	0.193	14.6	54.1	26.1

ϵ_{-5^*}. At $H_2=0.959$ T, the second anticrossing field, also the energy ϵ_{3^*} becomes lower than ϵ_{-5^*}, so that the transition $p(-5^*,3^*)$ appears (third column of Table I). At each anticrossing field a new transition occurs. The columns corresponding to $p(-5^*,2^*)$, $p(-5^*,1^*)$, and $p(-5^*,0^*)$ appear at $H_3=1.44$, $H_4=1.93$, and $H_5=2.41$ T, respectively. Note that $p(-5^*,5^*)$ is the main contribution for $0<H_z\lesssim 1$ T; $p(-5^*,4^*)$ dominates for $1.1\lesssim H_z\lesssim 1.5$ T and $p(-5^*,2^*)$ for $2\lesssim H_z\lesssim 2.7$ T.

The relaxation time vs field is shown in the semilogarithmic plot of Fig. 1. Two main features have to be pointed out: the large increasing of the relaxation time for $H_z\to 0$ and the deep downward spikes at the anticrossing fields $H_z=H_n$ with $n=5-m$ and $m=4,3,\ldots,0,-1$.

The growth of the relaxation time for $H_z\to 0$ is a consequence of the fact that $p(-5^*,5^*)$ is proportional to $(\epsilon_{-5^*}-\epsilon_{5^*})^3$, where $\epsilon_{-5^*}-\epsilon_{5^*}\simeq\sqrt{(\Delta_{-5,5})^2+(10g\mu_B H_z)^2}$ with $\Delta_{-5,5}/k_B=5.03\times10^{-7}$ K. For magnetic fields $H_z\gtrsim 10^{-7}$ T $(g\mu_B H_z\simeq\Delta_{-5,5})$ one has $\epsilon_{-5^*}-\epsilon_{5^*}\approx 10g\mu_B H_z$ and $\tau\approx(H_z)^{-3}$. For $H_z\lesssim 10^{-7}$ T, however, $\epsilon_{-5^*}-\epsilon_{5^*}\simeq\Delta_{-5,5}$ and $\tau\approx(\Delta_{-5,5})^{-3}$. In particular $\tau(0\text{ K},0\text{ T})=9.02\times10^{19}$ s. Any attempt to check this pseudodivergence at $H_z=0$ in the actual compound is prevented by the existence of local magnetic fields due to hyperfine and dipole interaction as discussed[9] for Mn_{12}. In the tetrairon cluster Fe_4 the hyperfine field should be $H_{\rm hyp}\lesssim 4\times10^{-5}$ T since only 2% of the natural iron has a nuclear spin $I=1/2$. From the crystal data[2] one estimates that the dipolar field between two Fe_4 molecules is $H_{\rm dip}\sim 4\times10^{-3}$ T that is 2 orders of magnitude greater than the hyperfine field. If we suppose that all six nearest-neighbor molecules Fe_4 have the magnetic moment directed along the positive z axis, a dipolar field on the order of $H_{\rm dip}\sim 0.025$ T is obtained. This should imply that at zero external field a transition to an ordered phase is expected at $T_{\rm dip}\sim 0.16$ K, which is not observed experimentally. So we think that the dipole-dipole interaction between Fe_4 molecules, neglected in our approach, may become dominant for $H_z\lesssim 0.01$ T for which we find $\tau(0\text{ K},0.01\text{ T})=5.37\times10^7$ s. The relaxation time in zero magnetic field shows a saturation[2] to a value of about 1500 s for $T\lesssim 0.2$ K. We obtain such a value for $H_z\approx 0.3$ T more than 1 order of magnitude greater than the expected dipolar field.

The deep downward spikes shown in Fig. 1 at the anticrossing fields are originated by the strong mixing of the states $|-5\rangle$ and $|m\rangle$ at $H_n\equiv H_{5-m}$ appearing in the eigenstate

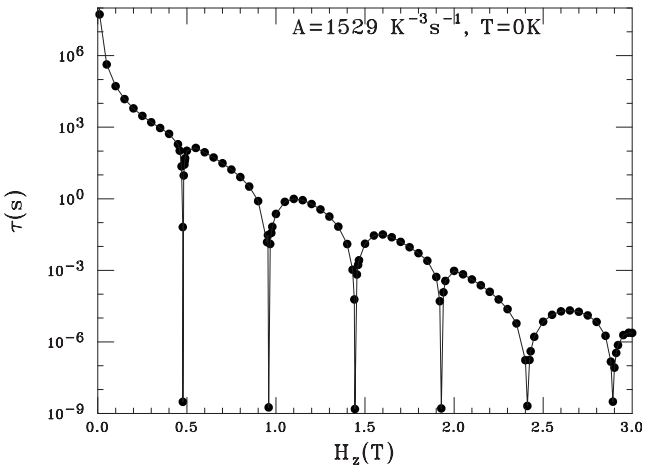

FIG. 1. Semilogarithmic plot of the relaxation time τ at $T=0$ K vs magnetic field for crystal-field parameters $B_2^0=-0.216$ K, $B_4^0=1.16\times10^{-5}$ K, $B_2^2=0.014$ K, and $B_4^3=7\times10^{-4}$ K.

$|-5^*\rangle$. In particular, the mixing concerns the states $|-5\rangle$ and $|4\rangle$ at H_1, $|-5\rangle$ and $|3\rangle$ at H_2, and so on. The strong mixing of the wave functions leads to a large increase in $p(-5^*,5^*)$ for $H_z\to H_1$ owing to the term $\langle 4|\{S_-,S_z\}|5\rangle$ in Eq. (19) and for $H_z\to H_2$ owing to the term $\langle 3|S_-^2|5\rangle$ in Eq. (19). Similarly the strong increase in $p(-5^*,4^*)$ for $H_z\to H_2$ and $H_z\to H_3$ is due to the terms $\langle 3|\{S_-,S_z\}|4\rangle$ and $\langle 2|S_-^2|4\rangle$, respectively. Similar considerations can be done for any $p(-5^*,m^*)$, so that a sudden decrease in the relaxation time is expected around any anticrossing magnetic fields. In the actual compound we think that the presence of hyperfine and dipolar field only spread the resonance about the anticrossing field but the spikes, possibly reduced, cannot disappear. We hope that a measure of the relaxation time of Fe_4 vs field at low temperature ($T\lesssim0.2$ K) may be done to check our expectation. Indeed such an experiment was done in Mn_{12} for $T\sim2$ K where resonance dips were recorded.[11]

IV. MASTER EQUATION

In this section we propose a GME that accounts for quantum tunneling at finite temperature taking advantage from the zero-temperature rigorous results of the previous section. To get the GME we use the master equation formalism[6] according to which the time evolution of the probability $\rho_{m^*}(t)$ of finding the molecule Fe_4 in the level $|m^*\rangle$ with energy ϵ_{m^*} at the time t is given by

$$\dot{\rho}_{m^*}=\sum_{n^*}W_{m^*,n^*}\rho_{n^*}-\rho_{m^*}\sum_{n^*}W_{n^*,m^*}. \tag{22}$$

As one can see from Eq. (22) the probability ρ_{m^*} increases in time owing to transitions from all other states $|n^*\rangle$ to $|m^*\rangle$ and decreases owing to transition from the state $|m^*\rangle$ to all other states $|n^*\rangle$. All transitions are ruled by the transition probability rates W_{n^*,m^*} given by Eq. (17). The standard master equation (SME) (Ref. 7) replaces $|m^*\rangle$ with $|m\rangle$ and ϵ_{m^*} with ϵ_m: the replacement of the eigenvalues and the eigenstates of the crystal-field Hamiltonian with the eigenvalues and the eigenstates of its diagonal part is justified by the fact that the nondiagonal terms are generally much smaller than the diagonal ones. Neglecting terms proportional to B_2^2 and B_4^3 in Eq. (2) the master Eq. (22) becomes

$$\dot{\rho}_m=\sum_n{}'W_{m,n}\rho_n-\rho_m\sum_n{}'W_{n,m}, \tag{23}$$

where $m=-5,\ldots,5$. The initial conditions are $\rho_m(0)=0$ for each $m\neq-5$ and $\rho_{-5}(0)=1$. The prime on the sum means that n is restricted to $n=m\pm1$, $m\pm2$. Indeed the nature of the spin-phonon interaction (8) makes all transition probability rates zero except

$$W_{m\pm1,m}=2A(2m\pm1)^2(5\mp m)(5\pm m+1)(\epsilon_{m\pm1}-\epsilon_m)^3n\left(\frac{\epsilon_{m\pm1}-\epsilon_m}{k_BT}\right) \tag{24}$$

and

$$W_{m\pm2,m}=A(5\mp m)(5\mp m-1)(5\pm m+1)(5\pm m+2)(\epsilon_{m\pm2}-\epsilon_m)^3n\left(\frac{\epsilon_{m\pm2}-\epsilon_m}{k_BT}\right). \tag{25}$$

The detailed set of $2S+1=11$ equations is given in the Appendix A. The ansatz

$$\rho_m(t)=\sum_{l=1}^{2S+1}r_m^{(l)}e^{\lambda_l t} \tag{26}$$

reduces the solution of the system of differential equations (23) to finding the $2S+1=11$ eigenvalues of the matrix $\boldsymbol{W}^{(0)}$ given by Eq. (A23). All the eigenvalues of the matrix $\boldsymbol{W}^{(0)}$ are *real* and *negative* except one, say λ_{11}, which is zero. This is consistent with the fact that for $t\to\infty$ all probabilities $\rho_m(t)$ must converge to their statistical equilibrium values,

$$\rho_m(t\to\infty)=r_m^{(11)}=\frac{e^{-\beta\epsilon_m}}{\sum_n e^{-\beta\epsilon_n}}. \tag{27}$$

The overall relaxation time is given by the reciprocal of the smallest (in magnitude) nonzero eigenvalue, say λ_{10}; that is,

$$\tau=\frac{1}{|\lambda_{10}|}. \tag{28}$$

At fixed magnetic field we see that the relaxation time vs temperature satisfies an Arrhenius law of the type

$$\tau(T,H_z)=\tau_0(H_z)e^{U(H_z)/T}, \tag{29}$$

where $U(H_z)$ is on the order of the energy barrier between the states $|\pm5\rangle$. From now on the energies are measured in kelvin. We find $\tau_0(H_z)=(3.1\pm0.1)\times10^{-8}$, $(4.3\pm0.2)\times10^{-8}$, and $(6.0\pm0.3)\times10^{-8}$ s and $U(H_z)=16.32\pm0.03$, 15.41 ± 0.05, and 14.06 ± 0.05 K for $H_z=0.05$, 0.2, and 0.4 T, respectively. Note that a fit of the data[2] with the Arrhenius law for $T\gtrsim1.9$ K and $H_z=0$ gives $\tau_0=(3.4\pm0.2)\times10^{-8}$ s and $U=15.6\pm0.2$ K. The Arrhenius law does not fit the experimental data for $T\lesssim1$ K and the relaxation time is found to saturate for $T\lesssim0.2$ K owing to quantum tunneling[2] in the presence of spin-phonon interaction.

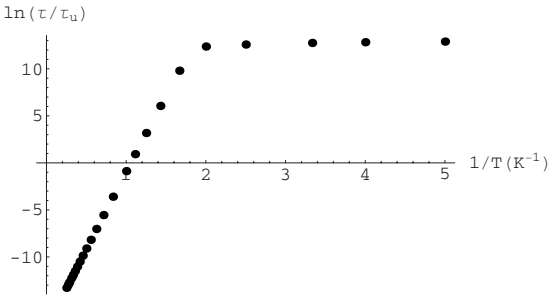

FIG. 2. Semilogarithmic plot of the relaxation time τ (s) and $\tau_u=1$ s for $H_z=0.05$ T vs the reciprocal of the temperature $1/T$ (K^{-1}) for $A=1529$ K^{-3} s^{-1}.

To account for quantum corrections at very low temperature we start with the master equation (22) keeping the most important quantum contribution deduced by Table I and Eq. (17). Since the transition probability rates $W_{m^*\pm1,m^*}$ and $W_{m^*\pm2,m^*}$ are the most important ones at finite temperature and they do not differ very much from the corresponding $W_{m\pm1,m}$ and $W_{m\pm2,m}$ we simply add the appropriate quantum transition probability rates $W_{m^*,-5^*}$ and W_{-5^*,m^*} to the SME of Eq. (23) leading to a GME. The selection of the transition probability rates is a consequence of the initial conditions of the experiment where each molecule is prepared in the state $|-5^*\rangle$ because of the application of a large negative magnetic field. Details of calculations are given in the Appendix B.

The relaxation time is the reciprocal of the smallest (in magnitude) nonzero eigenvalue λ_{10} of the matrix $\boldsymbol{W}^{(n)}$ with $n=1,2,\ldots,6$ given in Appendix B. Figure 2 shows the relaxation time vs temperature for $H_z=0.05$ T obtained from $\boldsymbol{W}^{(1)}$. As one can see the relaxation time follows an Arrhenius law for $T\gtrsim0.6$ K ($\tau=3.1\times10^{-8}e^{16.3/T}$ s) and saturates to the value $\tau=4.272\times10^5$ s for $T\to0$.

In Figs. 3–5 the relaxation time vs field is shown for $T=0.6$, 1, and 2 K, respectively. Full circles are obtained from

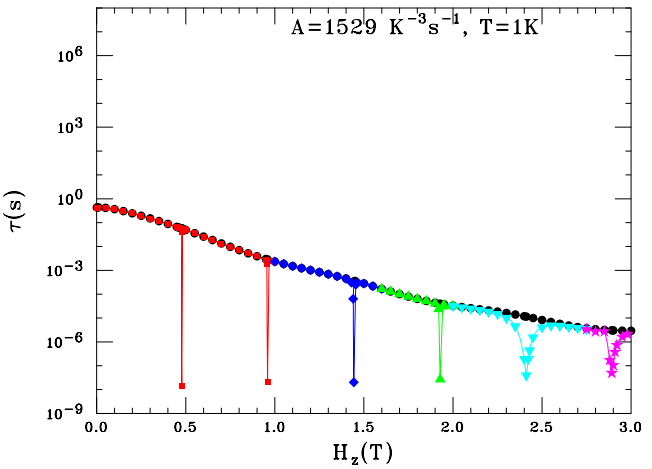

FIG. 4. (Color online) Semilogarithmic plot of the relaxation time τ at $T=1$ K vs magnetic field. Full (black) circles: SME; (red) squares: GME with $p(-5^*,5^*)$; (blue) diamonds: GME with $p(-5^*,4^*)$; (green) up triangles: GME master with $p(-5^*,3^*)$; (cyan) down triangles: GME with $p(-5^*,2^*)$; and (magenta) stars: GME with $p(-5^*,1^*)$.

the standard master equation corresponding to $\boldsymbol{W}^{(0)}$ (Appendix A); (red) squares are obtained from $\boldsymbol{W}^{(1)}(0<H_z<1$ T), where the quantum effect $p(-5^*,5^*)$ is taken into account (see Appendix B). For $1<H_z<1.6$ T we see from Table I that the dominant quantum contribution comes from $p(-5^*,4^*)$ and the matrix $\boldsymbol{W}^{(2)}$ is used to draw the (blue) diamonds. In the same way (green) up triangles ($1.6<H_z<2$ T), (cyan) down triangle ($2<H_z<2.7$ T), and (magenta) stars ($H_z>2.7$ T) are obtained accounting for $p(-5^*,3^*)$, $p(-5^*,2^*)$, and $p(-5^*,1^*)$ and making use of matrices $\boldsymbol{W}^{(3)}$, $\boldsymbol{W}^{(4)}$, and $\boldsymbol{W}^{(5)}$, respectively. The main discrepancies between the standard and quantum results are confined close to the anticrossing fields where the deep spikes found at $T=0$ K (see Fig. 1) are only slightly reduced. No trace of

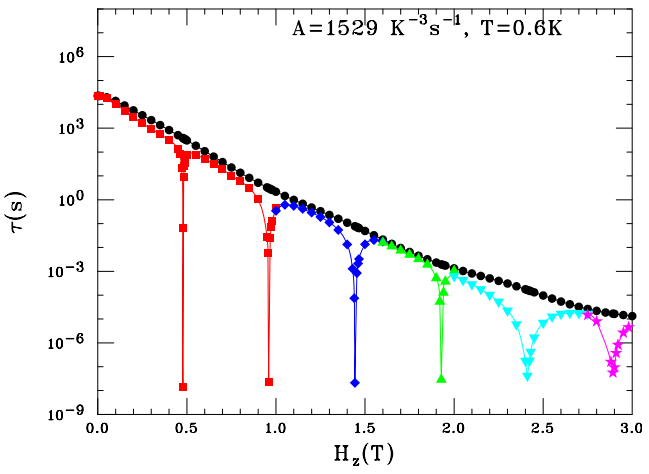

FIG. 3. (Color online) Semilogarithmic plot of the relaxation time τ at $T=0.6$ K vs magnetic field. Full (black) circles: SME; (red) squares: GME with $p(-5^*,5^*)$; (blue) diamonds: GME with $p(-5^*,4^*)$; (green) up triangles: GME with $p(-5^*,3^*)$; (cyan) down triangles: GME with $p(-5^*,2^*)$; and (magenta) stars: GME with $p(-5^*,1^*)$.

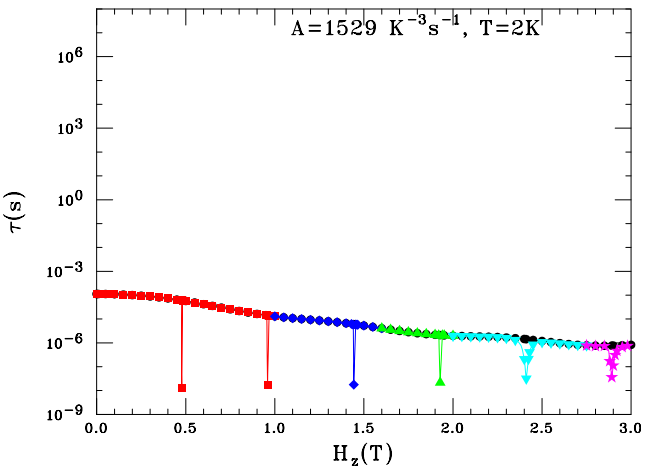

FIG. 5. (Color online) Semilogarithmic plot of the relaxation time τ at $T=2$ K vs magnetic field. Full (black) circles: SME; (red) squares: GME with $p(-5^*,5^*)$; (blue) diamonds: GME with $p(-5^*,4^*)$; (green) up triangles: GME with $p(-5^*,3^*)$; (cyan) down-triangles: GME with $p(-5^*,2^*)$; and (magenta) stars: GME with $p(-5^*,1^*)$.

the pseudodivergence for $H_z \to 0$ is obtained at variance with the zero-temperature result.

As one can see that at increasing temperature the relaxation time decreases and the width of the downward spikes shrinks, so that for temperature $T \simeq 2$ K only the spikes corresponding to the anticrossing fields H_5 and H_6 could be observed experimentally. For higher temperatures the thermally activated relaxation dominates the quantum tunneling effects.

For weak magnetic field and very low temperature, we are able to give an analytical expression for the total transition probability rate $W_{\rm tot}$. Indeed the leading terms that contribute to the depletion of the eigenstate $|-5^*\rangle$ come from the transitions to the states $|5^*\rangle$ and $|-4^*\rangle$; that is,

$$W_{\rm tot} \simeq W_{5^*,-5^*} + W_{-4^*,-5^*}, \tag{30}$$

where $W_{5^*,-5^*} \simeq Ap(-5^*,5^*)$ is small (see Table I) but finite, while

$$W_{-4^*,-5^*} \simeq W_{-4,-5} = 1.62 \times 10^3 A(5.77 - 1.34H_z)^3 n\left(\frac{5.77 - 1.34H_z}{T}\right) \tag{31}$$

goes to zero for $T \to 0$ owing to the occupation number. In Eq. (31) the energy is measured in kelvin and $g\mu_B/k_B$ is replaced with its value 1.34 K/T, so that the magnetic field H_z is measured in tesla. Note that the prefactor $p(-5,-4)$ is several orders of magnitude greater than $p(-5^*,5^*)$. For instance, for $H_z = 0.05$ T we have

$$W_{\rm tot} \simeq A\left[1.53 \times 10^{-9} + 3.01 \times 10^5 \; n\left(\frac{5.71}{T}\right)\right]. \tag{32}$$

Defining a crossover temperature T_0 between the quantum regime and the thermally activated one (where the relaxation time follows an Arrhenius law) as the temperature at which the two contributions are comparable, Eq. (32) gives $T_0 \simeq 0.17$ K in good agreement with the crossover temperature of the experiment.[2]

To get the relaxation time of Mn_{12} for $T \gtrsim 1$ K Leuenberger and Loss[10] proposed a different generalized master equation (LLME) in which phonon-induced spin transitions between levels ϵ_m and $\epsilon_{m\pm1}$ and between ϵ_m and $\epsilon_{m\pm2}$ as well as resonant tunneling caused by the nondiagonal part of the crystal-field Hamiltonian are taken into account. The LLME reads

$$\dot{\rho}_m = \frac{i}{\hbar}\langle m|[\rho, \mathcal{H}_{\rm cf}]|m\rangle + \sum_n{}' W_{m,n}\rho_n - \rho_m \sum_n{}' W_{n,m}, \tag{33}$$

where [,] is the commutator that accounts for quantum effects. A degenerate-level perturbation theory is applied to a suitable order to give a nonzero splitting between the two unperturbed levels with the same energy at the anticrossing field. A projection of the crystal-field Hamiltonian into the subspace of these two levels is then performed, so that the number of the off-diagonal elements generated by the commutation rules is drastically reduced. We apply the LLME to the tetrairon cluster Fe_4 restricting to $\rho_{-5,m}$ and $\rho_{m,-5}$, where $|-5\rangle$ and $|m\rangle$ are the crossing states at the field $H_n \equiv H_{5-m}$,

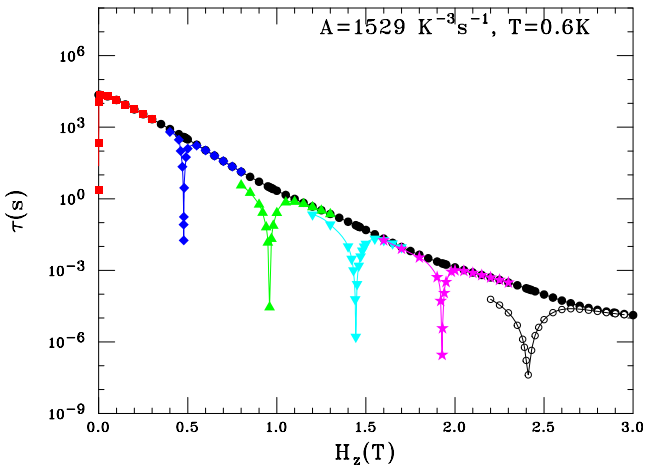

FIG. 6. (Color online) Semilogarithmic plot of the relaxation time τ at $T=0.6$ K vs magnetic field. Full (black) circles: SME; (red) squares: LLME with Γ^5_{-5}; (blue) diamonds: LLME with Γ^4_{-5}; (green) up triangles: LLME with Γ^3_{-5}; (cyan) down triangles: LLME with Γ^2_{-5}; (magenta) stars: LLME with Γ^1_{-5}; and open circles: LLME with Γ^0_{-5}.

and using an effective Hamiltonian as illustrated in the Appendix B. Taking advantage from the very short time decaying of the off-diagonal elements of the density matrix,[10] the LLME is obtained from the GME by replacing both W_{-5^*,m^*} and $W_{m^*,-5^*}$ appearing in GME with Γ^m_{-5}, where

$$\Gamma^m_{-5} = \left(\frac{\Delta_{-5,m}}{\hbar}\right)^2 \frac{\sum_n{}'(W_{n,m} + W_{n,-5})}{\left[\sum_n{}'(W_{n,m} + W_{n,-5})\right]^2 + \left[\frac{2g\mu_B H_z}{\hbar}(5+m)\right]^2}. \tag{34}$$

Note that $g\mu_B/\hbar = 1.76 \times 10^{11}$ (T s)$^{-1}$.

In Figs. 6–8 we show the relaxation time obtained from

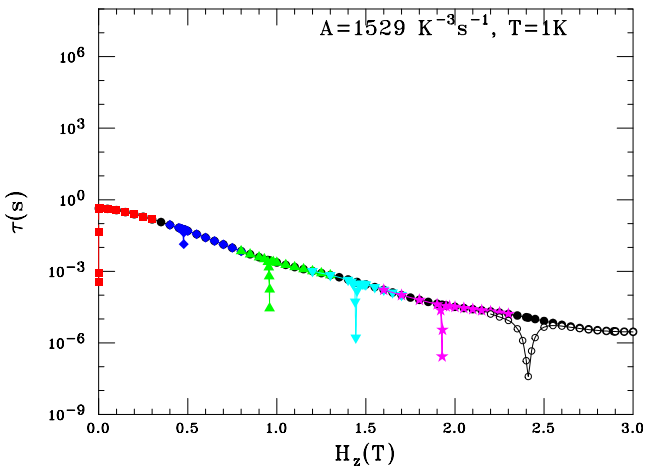

FIG. 7. (Color online) Semilogarithmic plot of the relaxation time τ at $T=1$ K vs magnetic field. Full (black) circles: SME; (red) squares: LLME with Γ^5_{-5}; (blue) diamonds: LLME with Γ^4_{-5}; (green) up triangles: LLME with Γ^3_{-5}; (cyan) down triangles: LLME with Γ^2_{-5}; (magenta) stars: LLME with Γ^1_{-5}; and open circles: LLME with Γ^0_{-5}.

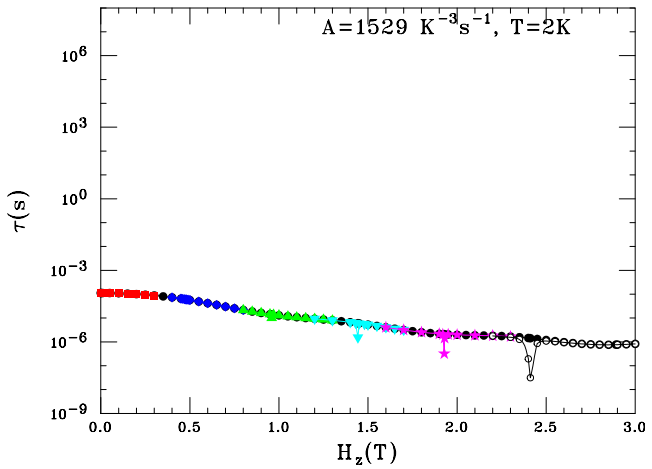

FIG. 8. (Color online) Semilogarithmic plot of the relaxation time τ at $T=2$ K vs magnetic field. Full (black) circles: SME; (red) squares: LLME with Γ^5_{-5}; (blue) diamonds: LLME with Γ^4_{-5}; (green) up triangles: LLME with Γ^3_{-5}; (cyan) down triangles: LLME with Γ^2_{-5}; (magenta) stars: LLME with Γ^1_{-5}; and open circles (○): LLME with Γ^0_{-5}.

the LLME of the Appendix B for $T=0.6$, 1, and 2 K, respectively. The SME result is shown for comparison using (black) full circles. The (red) squares, (blue) diamonds, (green) up triangles, (cyan) down triangles, (magenta) stars, and open circles are obtained from the LLME with Γ^5_{-5}, Γ^4_{-5}, Γ^3_{-5}, Γ^2_{-5}, Γ^1_{-5}, and Γ^0_{-5}, respectively.

Comparing Figs. 3 and 6, Figs. 4 and 7, and Figs. 5 and 8, an overall good agreement between the results obtained from the GME and LLME is seen. Spikes in correspondence of the anticrossing fields are found in both the GME and LLME. Quantitatively the spikes obtained from the GME are deeper than those obtained from the LLME. The main discrepancy is found at $H_z=0$, where the LLME leads to a downward spike for $T=0.6$ and 1 K, whereas in the GME no spike at all is found at $H_z=0$. This can be explained noticing that Γ^5_{-5} at low temperature and zero field is given by

$$\Gamma^5_{-5} \simeq \left(\frac{\Delta_{-5,5}}{\hbar}\right)^2 \frac{1}{2W_{4,5}} \simeq 5.31 e^{5.77/T} \ \text{s}^{-1}, \tag{35}$$

so that $\Gamma^5_{-5} \to \infty$ for $T \to 0$ and the relaxation time goes to zero. This seems to be an artifact of the approximation. Indeed for $T \to 0$ but $H_z \neq 0$ one has

$$\Gamma^5_{-5} \simeq \left(\frac{\Delta_{-5,5}}{\hbar}\right)^2 \frac{W_{4,5}}{2\left(\frac{10 g \mu_B H_z}{\hbar}\right)^2} \simeq 3.34 \times 10^{-7} \frac{e^{-\frac{5.77}{T}}}{H_z^2} \ \text{s}^{-1}, \tag{36}$$

so that $\Gamma^5_{-5} \to 0$ for $T \to 0$ leading to a divergent relaxation time. Such a result does not recover the quantum result according to which the relaxation time is finite at $T=0$ K. This inconvenience is not found for the other anticrossing fields. For instance at $H_z=H_1$ and low temperature Γ^4_{-5} saturates to the value

$$\Gamma^4_{-5} \simeq \left(\frac{\Delta_{-5,4}}{\hbar}\right)^2 \frac{1}{W_{5,4}} \simeq 10^2 \ \text{s}^{-1}, \tag{37}$$

so that $\tau \simeq 10^{-2}$ s. This saturation value seems to have been reached at $T=0.6$ K as shown in Fig. 6. For comparison the transition probability rate obtained directly from Eq. (21) is $W_{5^*,-5^*}=3.8\times10^8$ s^{-1}, so that $\tau \simeq 2.7\times10^{-9}$ s while at $T=0.6$, 1, and 2 K the relaxation time is $\tau \simeq 1.2-1.5 \times 10^{-8}$ s.

V. SUMMARY AND CONCLUSIONS

A theory that gives both the saturation of the relaxation time of the magnetization at very low temperature and the Arrhenius law at higher temperature has been formulated. A crucial role is played by the use of the eigenstates $|m^*\rangle$ of the crystal-field Hamiltonian instead of the eigenstates $|m\rangle$ of its diagonal part in the evaluation of the transition probability rates induced by the spin-phonon interaction. The use of the exact eigenstates allows us to obtain finite transition probability rates for $T \to 0$ owing to quantum tunneling. Moreover the master equation written in term of density-matrix elements on the basis $|m^*\rangle$ seems to be a very good starting point to obtain the relaxation time at finite temperature. An investigation of the transition probability rate at $T=0$ K allows us to simplify considerably the problem keeping only the dominant transition probability rate related to $p(-5^*,m^*)$, with the choice of m^* suggested by Table I. The choice of the main transition probability rate leads to a generalized master equation (GME) that recovers both the saturation of the relaxation time at low temperature and the Arrhenius law at higher temperature in agreement with the experiment on Fe_4. Also the crossover temperature between the two regimes is found to be in very good agreement with the experiment. The relaxation time versus field at $T=0$ shows deep downward spikes close to the anticrossing fields (see Fig. 1), a sign of the quantum tunneling at zero temperature. These spikes are present also at finite temperature as shown in Figs. 3–6. A problem arises around $H_z=0$ since the existence of hyperfine (weak in Fe_4) and dipolar fields prevents any check of the present theory for $H_z \lesssim 0.01$ T where the saturation value of the relaxation time, however, is orders of magnitude greater than that measured at $H_z=0$. Comparison between the GME and the generalized master equation proposed by Leuenberger and Loss[10] (LLME) to explain the field-dependent relaxation time of the magnetization in Mn_{12} for $T \gtrsim 2$ K gives a good qualitative agreement except for $H_z \approx 0$ as one can see comparing Figs. 3 and 4 with Figs. 6 and 7, respectively. For temperature $T \gtrsim 2$ K the discrepancy at $H_z \approx 0$ disappears as shown in Figs. 5 and 8. The quantitative agreement is not so good at the anticrossing fields. In any case the effect of the local fields should reduce and spread these resonances, so that quite similar quantitative values might be found in both theories. According to GME results the experimental check of the spikes at the anticrossing fields on the actual compound Fe_4 should be easier at temperature lower than $T \simeq 0.6$ K.

APPENDIX A: STANDARD MASTER EQUATIONS

In this appendix we give the explicit form of the master equations (23) for $Fe_4(S=5)$. The crystal-field parameters are $B_2^0=-0.216$, $B_4^0=1.16\times10^{-5}$ K, and $g\mu_B/k_B=1.34$ K/T. The eleven master equations are

$$\dot{\rho}_{-5} = W_{-5,-4}\rho_{-4} + W_{-5,-3}\rho_{-3} - (W_{-4,-5} + W_{-3,-5})\rho_{-5}, \tag{A1}$$

$$\dot{\rho}_{-4} = W_{-4,-5}\rho_{-5} + W_{-4,-3}\rho_{-3} + W_{-4,-2}\rho_{-2} - (W_{-5,-4} + W_{-3,-4} + W_{-2,-4})\rho_{-4}, \tag{A2}$$

$$\dot{\rho}_{-3} = W_{-3,-5}\rho_{-5} + W_{-3,-4}\rho_{-4} + W_{-3,-2}\rho_{-2} + W_{-3,-1}\rho_{-1} - (W_{-5,-3} + W_{-4,-3} + W_{-2,-3} + W_{-1,-3})\rho_{-3}, \tag{A3}$$

$$\dot{\rho}_{-2} = W_{-2,-4}\rho_{-4} + W_{-2,-3}\rho_{-3} + W_{-2,-1}\rho_{-1} + W_{-2,0}\rho_0 - (W_{-4,-2} + W_{-3,-2} + W_{-1,-2} + W_{0,-2})\rho_{-2}, \tag{A4}$$

$$\dot{\rho}_{-1} = W_{-1,-3}\rho_{-3} + W_{-1,-2}\rho_{-2} + W_{-1,0}\rho_0 + W_{-1,1}\rho_1 - (W_{-3,-1} + W_{-2,-1} + W_{0,-1} + W_{1,-1})\rho_{-1}, \tag{A5}$$

$$\dot{\rho}_0 = W_{0,-2}\rho_{-2} + W_{0,-1}\rho_{-1} + W_{0,1}\rho_1 + W_{0,2}\rho_2 - (W_{-2,0} + W_{-1,0} + W_{1,0} + W_{2,0})\rho_0, \tag{A6}$$

$$\dot{\rho}_1 = W_{1,-1}\rho_{-1} + W_{1,0}\rho_0 + W_{1,2}\rho_2 + W_{1,3}\rho_3 - (W_{-1,1} + W_{0,1} + W_{2,1} + W_{3,1})\rho_1, \tag{A7}$$

$$\dot{\rho}_2 = W_{2,0}\rho_0 + W_{2,1}\rho_1 + W_{2,3}\rho_3 + W_{2,4}\rho_4 - (W_{0,2} + W_{1,2} + W_{3,2} + W_{4,2})\rho_2, \tag{A8}$$

$$\dot{\rho}_3 = W_{3,1}\rho_1 + W_{3,2}\rho_2 + W_{3,4}\rho_4 + W_{3,5}\rho_5 - (W_{1,3} + W_{2,3} + W_{4,3} + W_{5,3})\rho_3, \tag{A9}$$

$$\dot{\rho}_4 = W_{4,2}\rho_2 + W_{4,3}\rho_3 + W_{4,5}\rho_5 - (W_{2,4} + W_{3,4} + W_{5,4})\rho_4, \tag{A10}$$

$$\dot{\rho}_5 = W_{5,3}\rho_3 + W_{5,4}\rho_4 - (W_{3,5} + W_{4,5})\rho_5, \tag{A11}$$

where

$$W_{-5,-4} = 1.62\times10^3 A(5.77-1.34H_z)^3\left[1 + n\left(\frac{5.77-1.34H_z}{T}\right)\right], \tag{A12}$$

$$W_{-5,-3} = 180A(10.3-2.68H_z)^3\left[1 + n\left(\frac{10.3-2.68H_z}{T}\right)\right], \tag{A13}$$

$$W_{-4,-3} = 1.76\times10^3 A(4.54-1.34H_z)^3\left[1 + n\left(\frac{4.54-1.34H_z}{T}\right)\right], \tag{A14}$$

$$W_{-4,-2} = 432A(7.80-2.68H_z)^3\left[1 + n\left(\frac{7.80-2.68H_z}{T}\right)\right], \tag{A15}$$

$$W_{-3,-2} = 1.20\times10^3 A(3.26-1.34H_z)^3\times\left[1 + n\left(\frac{3.26-1.34H_z}{T}\right)\right], \tag{A16}$$

$$W_{-3,-1} = 672A(5.23-2.68H_z)^3\left[1 + n\left(\frac{5.23-2.68H_z}{T}\right)\right], \tag{A17}$$

$$W_{-2,-1} = 504A(1.97-1.34H_z)^3\left[1 + n\left(\frac{1.97-1.34H_z}{T}\right)\right], \tag{A18}$$

$$W_{-2,0} = 840A(2.63-2.68H_z)^3\left[1 + n\left(\frac{2.63-2.68H_z}{T}\right)\right], \tag{A19}$$

$$W_{-1,0} = 60A(0.658-1.34H_z)^3\left[1 + n\left(\frac{0.658-1.34H_z}{T}\right)\right], \tag{A20}$$

$$W_{1,-1} = 900A(2.68H_z)^3\left[1 + n\left(\frac{2.68H_z}{T}\right)\right] \tag{A21}$$

with $n(x)=[e^x-1]^{-1}$, $A=1529$ K^{-3} s^{-1}, T in kelvin, and H_z in tesla. $W_{m,n}$ are obtained from $W_{n,m}$ by replacing $1+n(x)$ with $n(x)$ and $W_{m,n}$ are obtained from $W_{-m,-n}$ by replacing H_z with $-H_z$. The ansatz

$$\rho_m(t) = \sum_{l=1}^{11} r_m^{(l)} e^{\lambda_l t} \tag{A22}$$

reduces the solution of the system of differential equations (23) to an eigenvalue problem

$$\boldsymbol{W}^{(0)}\cdot\boldsymbol{r}^l = \lambda_l \boldsymbol{r}^l, \tag{A23}$$

where the nonzero elements of the tridiagonal matrix $\boldsymbol{W}^{(0)}$ are given by

$$\boldsymbol{W}_{1,1}^{(0)} = -W_{-4,-5} - W_{-3,-5}, \quad \boldsymbol{W}_{1,2}^{(0)} = W_{-5,-4}, \quad \boldsymbol{W}_{1,3}^{(0)} = W_{-5,-3}, \tag{A24}$$

$$\boldsymbol{W}_{2,1}^{(0)} = W_{-4,-5}, \quad \boldsymbol{W}_{2,2}^{(0)} = -W_{-5,-4} - W_{-3,-4} - W_{-2,-4}, \quad \boldsymbol{W}_{2,3}^{(0)} = W_{-4,-3}, \quad \boldsymbol{W}_{2,4}^{(0)} = W_{-4,-2}, \tag{A25}$$

$$W^{(0)}_{3,1} = W_{-3,-5}, \quad W^{(0)}_{3,2} = W_{-3,-4},$$

$$W^{(0)}_{3,3} = -W_{-5,-3} - W_{-4,-3} - W_{-2,-3} - W_{-1,-3},$$

$$W^{(0)}_{3,4} = W_{-3,-2}, \quad W^{(0)}_{3,5} = W_{-3,-1}, \tag{A26}$$

$$W^{(0)}_{4,2} = W_{-2,-4}, \quad W^{(0)}_{4,3} = W_{-2,-3},$$

$$W^{(0)}_{4,4} = -W_{-4,-2} - W_{-3,-2} - W_{-1,-2} - W_{0,-2},$$

$$W^{(0)}_{4,5} = W_{-2,-1}, \quad W^{(0)}_{4,6} = W_{-2,0}, \tag{A27}$$

$$W^{(0)}_{5,3} = W_{-1,-3}, \quad W^{(0)}_{5,4} = W_{-1,-2},$$

$$W^{(0)}_{5,5} = -W_{-3,-1} - W_{-2,-1} - W_{0,-1} - W_{1,-1},$$

$$W^{(0)}_{5,6} = W_{-1,0}, \quad W^{(0)}_{5,7} = W_{-1,1}, \tag{A28}$$

$$W^{(0)}_{6,4} = W_{0,-2}, \quad W^{(0)}_{6,5} = W_{0,-1},$$

$$W^{(0)}_{6,6} = -W_{-2,0} - W_{-1,0} - W_{1,0} - W_{2,0},$$

$$W^{(0)}_{6,7} = W_{0,1}, \quad W^{(0)}_{6,8} = W_{0,2}, \tag{A29}$$

$$W^{(0)}_{7,5} = W_{1,-1}, \quad W^{(0)}_{7,6} = W_{1,0},$$

$$W^{(0)}_{7,7} = -W_{-1,1} - W_{0,1} - W_{2,1} - W_{3,1},$$

$$W^{(0)}_{7,8} = W_{1,2}, \quad W^{(0)}_{7,9} = W_{1,3}, \tag{A30}$$

$$W^{(0)}_{8,6} = W_{2,0}, \quad W^{(0)}_{8,7} = W_{2,1},$$

$$W^{(0)}_{8,8} = -W_{0,2} - W_{1,2} - W_{3,2} - W_{4,2},$$

$$W^{(0)}_{8,9} = W_{2,3}, \quad W^{(0)}_{8,10} = W_{2,4}, \tag{A31}$$

$$W^{(0)}_{9,7} = W_{3,1}, \quad W^{(0)}_{9,8} = W_{3,2},$$

$$W^{(0)}_{9,9} = -W_{1,3} - W_{2,3} - W_{4,3} - W_{5,3},$$

$$W^{(0)}_{9,10} = W_{3,4}, \quad W^{(0)}_{9,11} = W_{3,5}, \tag{A32}$$

$$W^{(0)}_{10,8} = W_{4,2}, \quad W^{(0)}_{10,9} = W_{4,3},$$

$$W^{(0)}_{10,10} = -W_{2,4} - W_{3,4} - W_{5,4}, \quad W^{(0)}_{10,11} = W_{4,5}, \tag{A33}$$

$$W^{(0)}_{11,9} = W_{5,3}, \quad W^{(0)}_{11,10} = W_{5,4}, \quad W^{(0)}_{11,11} = -W_{3,5} - W_{4,5}, \tag{A34}$$

and the eigenvectors are column vectors given by $\boldsymbol{r}^l = (r^l_{-5}, r^l_{-4}, \ldots, r^l_4, r^l_5)$. Since $\Sigma_l W^{(0)}_{l,j} = 0$ for $j = 1, 2, \ldots, 11$, one of the eigenvalues, say λ_{11}, is zero.

APPENDIX B: GENERALIZED MASTER EQUATIONS (GME AND LLME)

To get the GME we account for the dominant quantum contributions coming from the transition probability rates neglected in the standard approach. As seen from Table I these contributions differ according to the magnetic field strength.

For $0 < H_z < 1$ T the dominant quantum contribution comes from $p(-5^*, 5^*)$, so that the only change concerns Eqs. (A1) and (A11) that become

$$\dot{\rho}_{-5} = W_{-5^*,5^*}\rho_5 + W_{-5,-4}\rho_{-4} + W_{-5,-3}\rho_{-3} - (W_{5^*,-5^*} + W_{-4,-5} + W_{-3,-5})\rho_{-5}, \tag{B1}$$

$$\dot{\rho}_5 = W_{5^*,-5^*}\rho_{-5} + W_{5,3}\rho_3 + W_{5,4}\rho_4 - (W_{-5^*,5^*} + W_{3,5} + W_{4,5})\rho_5, \tag{B2}$$

where

$$W_{5^*,-5^*} = Ap(-5^*, 5^*)\left[1 + n\left(\frac{\epsilon_{-5^*} - \epsilon_{5^*}}{T}\right)\right] \tag{B3}$$

and

$$W_{-5^*,5^*} = Ap(-5^*, 5^*)n\left(\frac{\epsilon_{-5^*} - \epsilon_{5^*}}{T}\right). \tag{B4}$$

The solution of the system is reduced to the evaluation of the eigenvalues and eigenvectors of the matrix $\boldsymbol{W}^{(1)}$ whose elements are the same as those of the matrix $\boldsymbol{W}^{(0)}$ except

$$W^{(1)}_{1,1} = -W_{-4,-5} - W_{-3,-5} - W_{5^*,-5^*}, \quad W^{(1)}_{1,11} = W_{-5^*,5^*} \tag{B5}$$

and

$$W^{(1)}_{11,1} = W_{5^*,-5^*}, \quad W^{(1)}_{11,11} = -W_{3,5} - W_{4,5} - W_{-5^*,5^*}. \tag{B6}$$

For $1 < H_z < 1.6$ T the dominant quantum contribution is $p(-5^*, 4^*)$; only Eqs. (A1) and (A10) are to be changed leading to the matrix $\boldsymbol{W}^{(2)}$ which has the same elements as $\boldsymbol{W}^{(0)}$ except

$$W^{(2)}_{1,1} = -W_{-4,-5} - W_{-3,-5} - W_{4^*,-5^*}, \quad W^{(2)}_{1,10} = W_{-5^*,4^*} \tag{B7}$$

and

$$W^{(2)}_{10,1} = W_{4^*,-5^*}, \quad W^{(2)}_{10,10} = -W_{2,4} - W_{3,4} - W_{5,4} - W_{-5^*,4^*}. \tag{B8}$$

For $1.6 < H_z < 2$ T the dominant quantum contribution is $p(-5^*, 3^*)$; only Eqs. (A1) and (A9) are to be changed leading to the matrix $\boldsymbol{W}^{(3)}$ which has the same elements as $\boldsymbol{W}^{(0)}$ except

$$W^{(3)}_{1,1} = -W_{-4,-5} - W_{-3,-5} - W_{3^*,-5^*}, \quad W^{(3)}_{1,9} = W_{-5^*,3^*} \tag{B9}$$

and

$$W^{(3)}_{9,1} = W_{3^*,-5^*}, \quad W^{(3)}_{9,9} = -W_{1,3} - W_{2,3} - W_{4,3} - W_{5,3} - W_{-5^*,3^*}. \tag{B10}$$

For $2 < H_z < 2.75$ T the dominant quantum contribution is $p(-5^*, 2^*)$; only Eqs. (A1) and (A8) are to be changed lead-

ing to the matrix $\boldsymbol{W}^{(4)}$ which has the same elements as $\boldsymbol{W}^{(0)}$ except

$$\boldsymbol{W}^{(4)}_{1,1} = -W_{-4,-5} - W_{-3,-5} - W_{2^*,-5^*}, \quad \boldsymbol{W}^{(4)}_{1,8} = W_{-5^*,2^*} \tag{B11}$$

and

$$\boldsymbol{W}^{(4)}_{8,1} = W_{2^*,-5^*},$$

$$\boldsymbol{W}^{(4)}_{8,8} = -W_{0,2} - W_{1,2} - W_{3,2} - W_{4,2} - W_{-5^*,2^*}. \tag{B12}$$

For $2.75 < H_z < 3$ T the dominant quantum contribution is $p(-5^*, 1^*)$; only Eqs. (A1) and (A7) are to be changed leading to the matrix $\boldsymbol{W}^{(5)}$ which has the same elements as $\boldsymbol{W}^{(0)}$ except

$$\boldsymbol{W}^{(5)}_{1,1} = -W_{-4,-5} - W_{-3,-5} - W_{1^*,-5^*}, \quad \boldsymbol{W}^{(5)}_{1,7} = W_{-5^*,1^*} \tag{B13}$$

and

$$\boldsymbol{W}^{(5)}_{7,1} = W_{1^*,-5^*},$$

$$\boldsymbol{W}^{(5)}_{7,7} = -W_{-1,1} - W_{0,1} - W_{2,1} - W_{3,1} - W_{-5^*,1^*}. \tag{B14}$$

Finally for $H_z > 3$ T the dominant quantum contribution is $p(-5^*, 0^*)$; only Eqs. (A1) and (A6) are to be changed leading to the matrix $\boldsymbol{W}^{(6)}$ which has the same elements as $\boldsymbol{W}^{(0)}$ except

$$\boldsymbol{W}^{(6)}_{1,1} = -W_{-4,-5} - W_{-3,-5} - W_{0^*,-5^*}, \quad \boldsymbol{W}^{(6)}_{1,6} = W_{-5^*,0^*} \tag{B15}$$

and

$$\boldsymbol{W}^{(6)}_{6,1} = W_{0^*,-5^*},$$

$$\boldsymbol{W}^{(6)}_{6,6} = -W_{-2,0} - W_{-1,0} - W_{1,0} - W_{2,0} - W_{-5^*,0^*}. \tag{B16}$$

Since $\Sigma_l \boldsymbol{W}^{(n)}_{l,j} = 0$ for $j = 1, 2, \ldots, 11$, one of the eigenvalues of each matrix $\boldsymbol{W}^{(n)}$ with $n = 1, 2, \ldots, 6$ is zero.

A different generalized master equation (LLME) was proposed by Leuenberger and Loss.[10] They replace m^* with m in the phonon-induced transition probability rate treating quantum tunneling in a perturbative way. In the LLME the differential equations for the diagonal and off-diagonal elements of the density matrix are

$$\dot{\rho}_m = \frac{i}{\hbar}\langle m|[\rho, \mathcal{H}_{\rm cf}]|m\rangle + \sum_n W_{m,n}\rho_n - \rho_m \sum_n W_{n,m} \tag{B17}$$

and

$$\dot{\rho}_{m,m'} = \frac{i}{\hbar}\langle m|[\rho, \mathcal{H}_{\rm cf}]|m'\rangle - \frac{1}{2}\rho_{m,m'}\sum_n (W_{n,m} + W_{n,m'}), \tag{B18}$$

respectively, with $m, m' = -5, \ldots, 5$ and $m \neq m'$. The off-diagonal elements are originated from the choice of the eigenstates $|m\rangle$ that are not eigenstates of the crystal-field Hamiltonian (1). The systems (B17) and (B18) have $2S+1 = 11$ and $2S(2S+1) = 110$ equations, respectively. This number is drastically reduced if one assumes[10] that the crystal-field Hamiltonian $\mathcal{H}_{\rm cf}$ may be replaced with its projection on the two-state system $|m\rangle, |m'\rangle$ corresponding to the two levels of the diagonal part of the Hamiltonian that are degenerate at the anticrossing field $H_n^{(0)}$. The elements of the projected Hamiltonian are

$$\langle m|\mathcal{H}_{\rm cf}|m\rangle = \epsilon_m(H_n^{(0)}) - g\mu_B m(H_z - H_n^{(0)}), \tag{B19}$$

$$\langle m'|\mathcal{H}_{\rm cf}|m\rangle = \langle m|\mathcal{H}_{\rm cf}|m'\rangle = \frac{1}{2}\Delta^{(0)}_{m,m'}(H_n^{(0)}), \tag{B20}$$

where $\Delta^{(0)}_{m,m'}(H_n^{(0)})$ is the splitting between levels $\epsilon_m(H_n^{(0)}) = \epsilon_{m'}(H_n^{(0)})$ at the anticrossing field. This splitting is to be evaluated by means of the time-independent degenerate-level perturbation theory pushed to a convenient order to give $\Delta^{(0)}_{m,m'} \neq 0$. For the tetrairon cluster Fe_4 the perturbation Hamiltonian is $V = B_2^2 O_2^2 + B_4^3 O_4^3$. For $m = -5$ and $m' = 5$ ($H_0^{(0)} = 0$) the chain formula[9,10] for the splitting $\Delta^{(0)}_{-5,5}$ is the sum of seven contributions: one corresponding to the chain formed by five potential $B_2^2 O_2^2$ and the other six contributions coming from all permutations of two potentials $B_2^2 O_2^2$ and two potentials $B_4^3 O_4^3$. This gives $\Delta^{(0)}_{-5,5} = 8.83(B_2^2)^5 + 5.29 \times 10^3 (B_2^2)^2 (B_4^3)^2 = 5.12 \times 10^{-7}$ K. For $m = -5$ and $m' = 4$ ($H_1^{(0)} = 0.478$ T) one obtains $\Delta^{(0)}_{-5,4} = 8.96 \times 10^2 (B_2^2)^3 B_4^3 + 9.21 \times 10^3 (B_4^3)^3 = 4.88 \times 10^{-6}$ K. For $m = -5$ and $m' = 3$ ($H_2^{(0)} = 0.959$ T) one obtains $\Delta^{(0)}_{-5,3} = 53.9(B_2^2)^4 + 7.33 \times 10^3 B_2^2 (B_4^3)^2 = 5.23 \times 10^{-5}$ K. For $m = -5$ and $m' = 2$ ($H_3^{(0)} = 1.44$ T) one has $\Delta^{(0)}_{-5,2} = 1.59 \times 10^3 (B_2^2)^2 B_4^3 = 2.18 \times 10^{-4}$ K. For $m = -5$ and $m' = 1$ ($H_4^{(0)} = 1.93$ T) one has $\Delta^{(0)}_{-5,1} = 98.2(B_2^2)^3 + 1.57 \times 10^3 (B_4^3)^2 = 1.04 \times 10^{-3}$ K. For $m = -5$ and $m' = 0$ ($H_5^{(0)} = 2.41$ T) one has $\Delta^{(0)}_{-5,0} = 1.24 \times 10^3 B_2^2 B_4^3 = 1.21 \times 10^{-2}$ K.

A quite similar result is obtained by replacing the crystal-field Hamiltonian with a two-level effective Hamiltonian[4] $\mathcal{H}_{\rm eff}$ connecting only the two states that are mixed at the anticrossing field H_n; that is,

$$\mathcal{H}_{\rm eff} = \begin{pmatrix} \epsilon_{-5}(H_n) + 5g\mu_B(H_z - H_n) & \frac{1}{2}\Delta_{-5,m}(H_n) \\ \frac{1}{2}\Delta_{-5,m}(H_n) & \epsilon_m(H_n) - mg\mu_B(H_z - H_n) \end{pmatrix} \tag{B21}$$

where the energy splitting and anticrossing fields were taken from the diagonalization of the complete spin Hamiltonian. In particular, one obtains $\Delta_{-5,5}(0) = 5.03 \times 10^{-7}$ K for $H_z = 0$, $\Delta_{-5,4} = 1.46 \times 10^{-6}$ K for $H_1 = 0.477$ T, $\Delta_{-5,3} = 4.82 \times 10^{-5}$ K for $H_2 = 0.959$ T, $\Delta_{-5,2} = 2.18 \times 10^{-4}$ K for $H_3 = 1.44$ T, $\Delta_{-5,1} = 5.05 \times 10^{-4}$ K for $H_4 = 1.93$ T, and $\Delta_{-5,0} = 1.21 \times 10^{-2}$ K for $H_5 = 2.41$ T. As one can see the agreement between these two approaches is very good as for the values of the anticrossing fields. Not so good is the agreement for the splittings even though the order of magnitude is recovered by the perturbation result. The overestimate is out-

standing for $\Delta_{-5,4}$ and $\Delta_{-5,1}$. We use the effective Hamiltonian to write the LLME.

For magnetic field $H_z \approx 0$ the two-state subspace is spanned by $|-5\rangle$ and $|5\rangle$, so that Eq. (B17) gives

$$\dot{\rho}_{-5} = \frac{i}{2\hbar}\Delta_{-5,5}(\rho_{-5,5} - \rho_{5,-5}) + W_{-5,-4}\rho_{-4} + W_{-5,-3}\rho_{-3} - (W_{-4,-5} + W_{-3,-5})\rho_{-5}, \tag{B22}$$

$$\dot{\rho}_5 = \frac{i}{2\hbar}\Delta_{-5,5}(\rho_{5,-5} - \rho_{-5,5}) + W_{5,4}\rho_4 + W_{5,3}\rho_3 - (W_{4,5} + W_{3,5})\rho_5, \tag{B23}$$

while the equations for $\dot{\rho}_n$ with $n \neq -5, 5$ are given by Eqs. (A2)–(A10). Analogously Eq. (B18) gives

$$\dot{\rho}_{5,-5} = \frac{i}{\hbar}(10g\mu_B H_z)\rho_{5,-5} + \frac{i}{2\hbar}\Delta_{-5,5}(\rho_5 - \rho_{-5}) - \frac{1}{2}(W_{3,5} + W_{4,5} + W_{-3,-5} + W_{-4,-5})\rho_{5,-5} \tag{B24}$$

and

$$\dot{\rho}_{-5,5} = -\frac{i}{\hbar}(10g\mu_B H_z)\rho_{-5,5} + \frac{i}{2\hbar}\Delta_{-5,5}(\rho_{-5} - \rho_5) - \frac{1}{2}(W_{3,5} + W_{4,5} + W_{-3,-5} + W_{-4,-5})\rho_{-5,5}. \tag{B25}$$

Under the assumption[10] that the overall relaxation time is much longer than the time of decaying of the off-diagonal elements one can neglect their time dependence and take the solutions of Eqs. (B24) and (B25) for $\dot{\rho}_{-5,5} = \dot{\rho}_{5,-5} = 0$. So doing one obtains

$$\rho_{5,-5} = \frac{\frac{i}{2\hbar}\Delta_{-5,5}(\rho_5 - \rho_{-5})}{\frac{1}{2}(W_{3,5} + W_{4,5} + W_{-3,-5} + W_{-4,-5}) - \frac{i}{\hbar}(10g\mu_B H_z)} \tag{B26}$$

and $\rho_{-5,5}$ is the complex conjugate of $\rho_{5,-5}$. Replacing the off-diagonal terms obtained in Eqs. (B22) and (B23) one obtains

$$\dot{\rho}_{-5} = \Gamma^5_{-5}\rho_5 + W_{-5,-4}\rho_{-4} + W_{-5,-3}\rho_{-3} - (\Gamma^5_{-5} + W_{-4,-5} + W_{-3,-5})\rho_{-5} \tag{B27}$$

and

$$\dot{\rho}_5 = \Gamma^5_{-5}\rho_{-5} + W_{5,4}\rho_4 + W_{5,3}\rho_3 - (\Gamma^5_{-5} + W_{4,5} + W_{3,5})\rho_5, \tag{B28}$$

where

$$\Gamma^5_{-5} = \left(\frac{\Delta_{-5,5}}{\hbar}\right)^2 \frac{W_{3,5} + W_{4,5} + W_{-3,-5} + W_{-4,-5}}{(W_{3,5} + W_{4,5} + W_{-3,-5} + W_{-4,-5})^2 + \left(\frac{20g\mu_B H_z}{\hbar}\right)^2}. \tag{B29}$$

Note that Eqs. (B27) and (B28) reduce to Eqs. (B1) and (B2) if one replaces both $W_{-5^*,5^*}$ and $W_{5^*,-5^*}$ with Γ^5_{-5}. In this way we obtain directly from Eqs. (B5) and (B6) the matrix $\overline{W}^{(1)}$ and use the same procedure illustrated in the Appendix A to find the relaxation time.

For $H_z \approx H_1$ the crystal-field Hamiltonian is projected on the two-state subspace $|-5\rangle, |4\rangle$ and we obtain the matrix $\overline{W}^{(2)}$ by replacing both $W_{-5^*,4^*}$ and $W_{4^*,-5^*}$ in Eqs. (B7) and (B8) with Γ^4_{-5}, where

$$\Gamma^4_{-5} = \left(\frac{\Delta_{-5,4}}{\hbar}\right)^2 \frac{W_{2,4} + W_{3,4} + W_{5,4} + W_{-3,-5} + W_{-4,-5}}{(W_{2,4} + W_{3,4} + W_{5,4} + W_{-3,-5} + W_{-4,-5})^2 + \left[\frac{18g\mu_B(H_z - H_1)}{\hbar}\right]^2}. \tag{B30}$$

For $H_z \approx H_2$ the matrix $\overline{W}^{(3)}$ is obtained by replacing both $W_{-5^*,3^*}$ and $W_{3^*,-5^*}$ in Eqs. (B9) and (B10) with Γ^3_{-5}, where

$$\Gamma^3_{-5} = \left(\frac{\Delta_{-5,3}}{\hbar}\right)^2 \frac{W_{1,3} + W_{2,3} + W_{4,3} + W_{5,3} + W_{-3,-5} + W_{-4,-5}}{(W_{1,3} + W_{2,3} + W_{4,3} + W_{5,3} + W_{-3,-5} + W_{-4,-5})^2 + \left[\frac{16g\mu_B(H_z - H_2)}{\hbar}\right]^2}. \tag{B31}$$

For $H_z \approx H_3$ the matrix $\overline{W}^{(4)}$ is obtained by replacing both $W_{-5^*,2^*}$ and $W_{2^*,-5^*}$ in Eqs. (B11) and (B12) with Γ^2_{-5}, where

$$\Gamma^2_{-5} = \left(\frac{\Delta_{-5,2}}{\hbar}\right)^2 \frac{W_{0,2} + W_{1,2} + W_{3,2} + W_{4,2} + W_{-3,-5} + W_{-4,-5}}{(W_{0,2} + W_{1,2} + W_{3,2} + W_{4,2} + W_{-3,-5} + W_{-4,-5})^2 + \left[\frac{14g\mu_B(H_z - H_3)}{\hbar}\right]^2}. \tag{B32}$$

For $H_z \approx H_4$ the matrix $\overline{W}^{(5)}$ is obtained by replacing both $W_{-5^*,1^*}$ and $W_{1^*,-5^*}$ in Eqs. (B13) and (B14) with Γ^1_{-5}, where

$$\Gamma^1_{-5} = \left(\frac{\Delta_{-5,1}}{\hbar}\right)^2 \frac{W_{-1,1} + W_{0,1} + W_{2,1} + W_{3,1} + W_{-3,-5} + W_{-4,-5}}{(W_{-1,1} + W_{0,1} + W_{2,1} + W_{3,1} + W_{-3,-5} + W_{-4,-5})^2 + \left[\frac{12g\mu_B(H_z - H_4)}{\hbar}\right]^2}. \tag{B33}$$

For $H_z \approx H_5$ the matrix $\overline{W}^{(6)}$ is obtained by replacing both $W_{-5^*,0^*}$ and $W_{0^*,-5^*}$ in Eqs. (B15) and (B16) with Γ^0_{-5}, where

$$\Gamma_{-5}^{0} = \left(\frac{\Delta_{-5,0}}{\hbar}\right)^2 \frac{W_{-2,0} + W_{-1,0} + W_{1,0} + W_{2,0} + W_{-3,-5} + W_{-4,-5}}{(W_{-1,1} + W_{0,1} + W_{2,1} + W_{3,1} + W_{-3,-5} + W_{-4,-5})^2 + \left[\frac{10 g \mu_B (H_z - H_5)}{\hbar}\right]^2}. \tag{B34}$$

*Also at Istituto IMEM of CNR, Parco Area delle Scienze, 43100 Parma, Italy; rastelli@fis.unipr.it

[1] D. Gatteschi, R. Sessoli, and J. Villain, *Molecular Nanomagnets* (Oxford University Press, Oxford, 2006).

[2] A. Cornia, A. C. Fabretti, P. Garrisi, C. Mortalò, D. Bonacchi, D. Gatteschi, R. Sessoli, L. Sorace, W. Wernsdorfer, and A. L. Barra, Angew. Chem., Int. Ed. **43**, 1136 (2004).

[3] S. Carretta, P. Santini, G. Amoretti, T. Guidi, R. Caciuffo, A. Candini, A. Cornia, D. Gatteschi, M. Plazanet, and J. A. Stride, Phys. Rev. B **70**, 214403 (2004).

[4] E. Rastelli and A. Tassi, Phys. Rev. B **75**, 134414 (2007).

[5] R. A. Klemm and D. V. Efremov, Phys. Rev. B **77**, 184410 (2008).

[6] K. Blum, *Density Matrix Theory and Applications* (Plenum, New York, 1981).

[7] J. Villain, F. Hartmann-Boutron, R. Sessoli, and A. Rettori, Europhys. Lett. **27**, 159 (1994).

[8] R. Sessoli, D. Gatteschi, A. Caneschi, and M. A. Novak, Nature (London) **365**, 141 (1993).

[9] F. Hartmann-Boutron, P. Politi, and J. Villain, Int. J. Mod. Phys. B **10**, 2577 (1996); P. Politi, A. Rettori, F. Hartmann-Boutron, and J. Villain, Phys. Rev. Lett. **75**, 537 (1995).

[10] M. N. Leuenberger and D. Loss, Phys. Rev. B **61**, 1286 (2000).

[11] L. Thomas, F. Lionti, R. Ballou, D. Gatteschi, R. Sessoli, and B. Barbara, Nature (London) **383**, 145 (1996); F. Lionti, L. Thomas, R. Ballou, B. Barbara, A. Sulpice, R. Sessoli, and D. Gatteschi, J. Appl. Phys. **81**, 4608 (1997); S. W. Yoon, M. Heu, W. S. Jeon, D. Y. Jung, B. J. Suh, and S. Yoon, Phys. Rev. B **67**, 052402 (2003).

[12] M. T. Hutchings, in *Solid State Physics*, edited by F. Seitz and D. Turnbull (Academic Press, New York, 1964), Vol. 16, p. 227.

[13] E. Callen and H. B. Callen, Phys. Rev. **139**, A455 (1965).